VOLUME 1 NUMBER 1 1992

Nanobiology

JOURNAL OF RESEARCH ON
NANOSCALE LIVING SYSTEMS

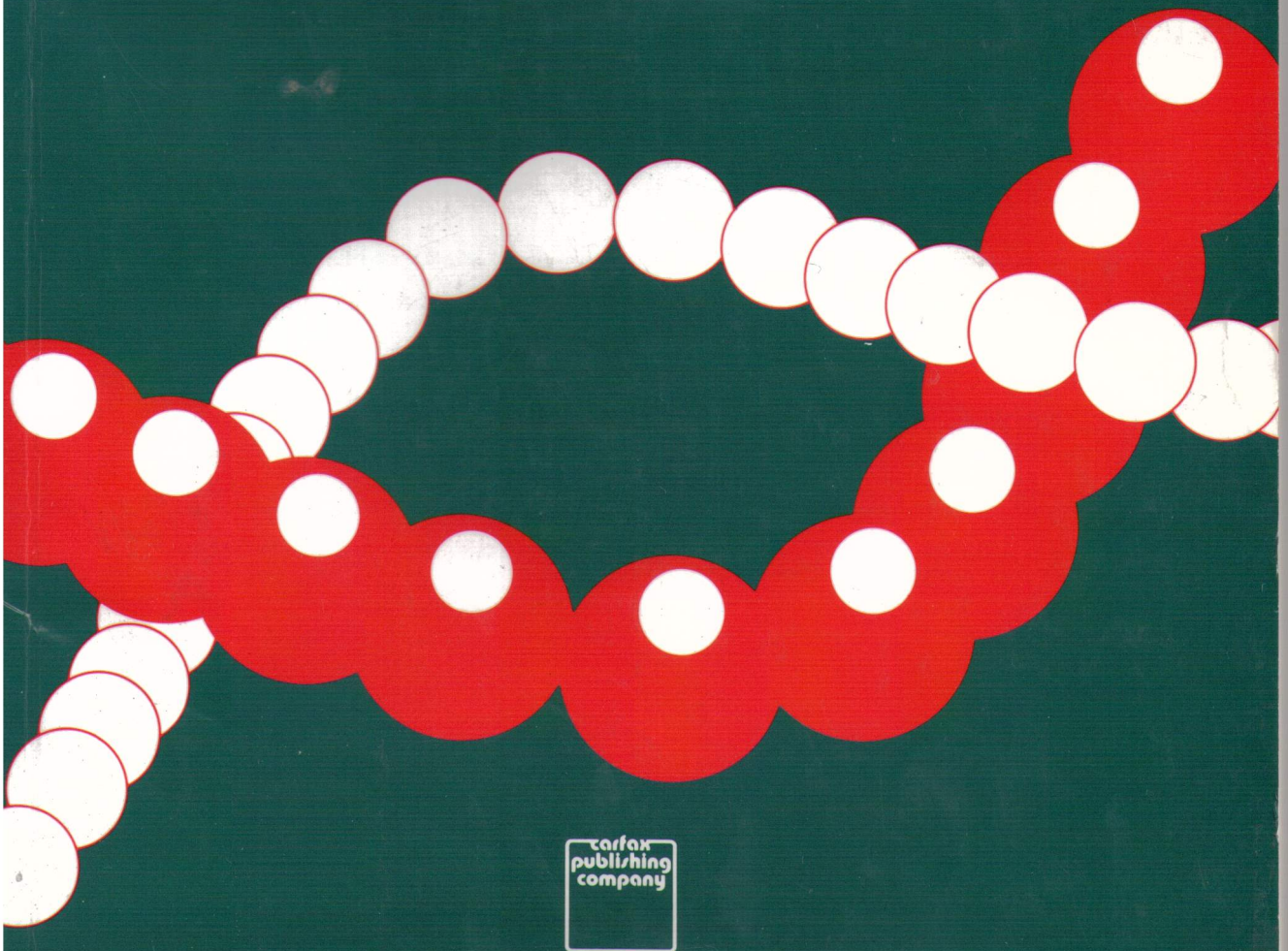

taylor & francis
publishing
company

ISSN 0958-3165

Nanobiology

VOLUME 1 NUMBER 1 1992

Nanobiology (1992) *1*, 61–74

Microtubule Dynamics, Liposomes and Artificial Cells: *in vitro* Observation and Cellular Automata Simulation of Microtubule Assembly/Disassembly and Membrane Morphogenesis

HIROKAZU HOTANI,[1*] RAFAEL LAHOZ-BELTRA,[2†] BRIAN COMBS,[3] STUART HAMEROFF[2] AND STEEN RASMUSSEN[3]

[1]ERATO Molecular Dynamic Assembly, 15 Morimoto-cho, Shimogamo, Sakyo-ku, Kyoto 606, Japan; [2]Advanced Biotechnology Laboratory, Department of Anesthesiology, The University of Arizona Health Sciences Center, Tucson, AZ 85724, USA; [3]Center for Non-linear Studies and Theoretical Division (T-13), MS-B258, Los Alamos National Laboratory, Los Alamos, NM 87545, USA

Adaptive and purposeful behaviors within cells (locomotion, phagocytosis, pseudopod formation, growth, trophism, synaptic plasticity, axoplasmic transport) can apparently occur in real time without immediate genetic control. Rather, these functional activities depend to a great extent on intracellular dynamics governed by the cytoskeleton: networks of filamentous protein polymers. The architecture of cytoskeletal networks and control of form and function in eukaryotic cells depend primarily on the assembly, disassembly and interconnection of cytoskeletal microtubules (MTs) and filaments.

In this paper we focus on MTs. We present in vitro *observation and two types of cellular automata computer simulation of MT assembly/disassembly. Erratic oscillations between phases of MT assembly and disassembly (dynamic instability) and concurrent assembly at one end and disassembly at the opposite end of single MT (treadmilling) are observed both* in vitro *and in cellular automata computer simulation. We also report on* in vitro *observation of MT polymerizing within liposome membrane spheres, causing marked deformation and extension of the liposome surface. Thus, this paper describes several dynamic activities of cytoskeletal MTs and MT/membranes whose non-linear behaviors are closely simulated by cellular automata models based on biophysical interactions of MT subunit proteins.*

INTRODUCTION

Roots of cognition within living systems—self-organization, communication, information processing and adaptive, purposeful behaviors—originate at the level of biomolecular systems *within* cells, and often occur too rapidly to involve genetic control. Such behavior includes

Correspondence to Stuart Hameroff or Steen Rasmussen.

*Present address: School of Science and Engineering, Teikyo University, 1-1 Toyosatodai, Utsunomiya 320, Japan.

†Permanent address: Department of Applied Mathematics, Faculty of Biological Sciences, Complutense University of Madrid, Madrid 28040, Spain. Dr Lahoz-Beltre was supported by a Fulbright/Ministerio de Educacion y Ciencia (Spain) award presented in 1989.

cytoplasmic locomotion, phagocytosis, pseudopod formation, growth, trophism, synaptic plasticity and axoplasmic transport, and are controlled by dynamic activities of the cytoskeleton—networks of interconnected protein polymers including microtubules (MTs), intermediate filaments, actin, microtubule-associated proteins (MAPs) and others (Figures 1 and 2). In addition to bone-like structural support, the cytoskeleton appears to be the internal nervous system of the cell (Hameroff, 1987; Rasmussen *et al.*, 1990). Assembly and disassembly of cytoskeletal MTs, in particular, describe cellular form and function (Lennon *et al.*, 1980). In this paper we describe both direct observation and computer simulation of several aspects of MT assembly/disassembly.

The direct observation of MT assembly/disassembly utilizes dark-field video microscopy to image dynamically individual MTs growing, shrinking and treadmilling (Horio & Hotani, 1986). Such observations confirm theoretical predictions of MT behavior (Kirschner & Mitchison, 1986). As an initial step in studying the role of MTs in morphogenesis of biological cells, the direct observation reported in this paper includes polymerization of MTs inside spherical lipid vesicles called liposomes. MT assembly causes marked extension and deformation of the lipid membrane—similar to neurite extension in a developing neuron. Although this phenomenon was not directly modeled, it is included because it may presage development of artificial cells.

Cellular automata are computer simulation techniques in which interactive components are directly represented, their dynamics being determined by rules governing component interactions. Thus, cellular automata are 'microscopic' modeling techniques which have clear advantages over more traditional 'macroscopic' approaches such as differential equations because the physical processes can be modeled more directly. Using cellular automata to simulate phenomena such as MT assembly/disassembly, model structure and parameters can be directly related to molecular mechanisms and biophysical properties. In this paper, we utilize two types of cellular automata techniques: a stochastic cellular automata model in which each subunit protein is considered to be in a finite number of states, and a movable finite automata model in which bond site strengths, free energy and conformational states may be considered. Similarities in MT behavior among both types of automata simulation and direct *in vitro* observation suggest that basic logic and rules governing MT assembly/disassembly have been captured in the automata models.

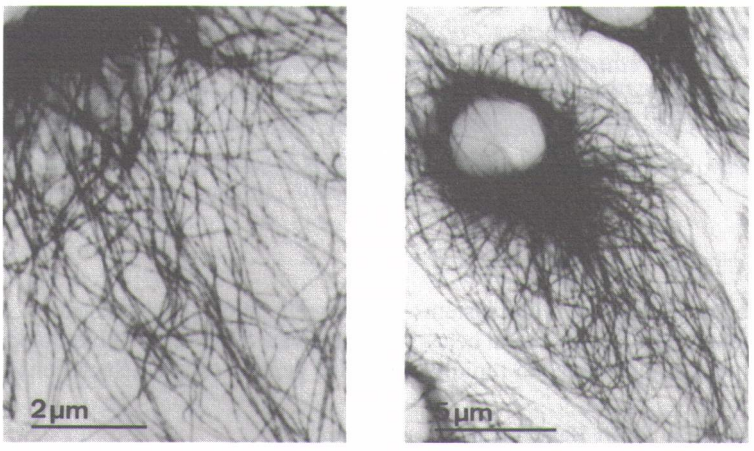

FIGURE 1. Tissue culture cells illustrating microtubules (MT) by dark staining immunofluorescence. Dense arrays of MT near nucleus emanate from centrioles. With permission from Geuens *et al.* (1986).

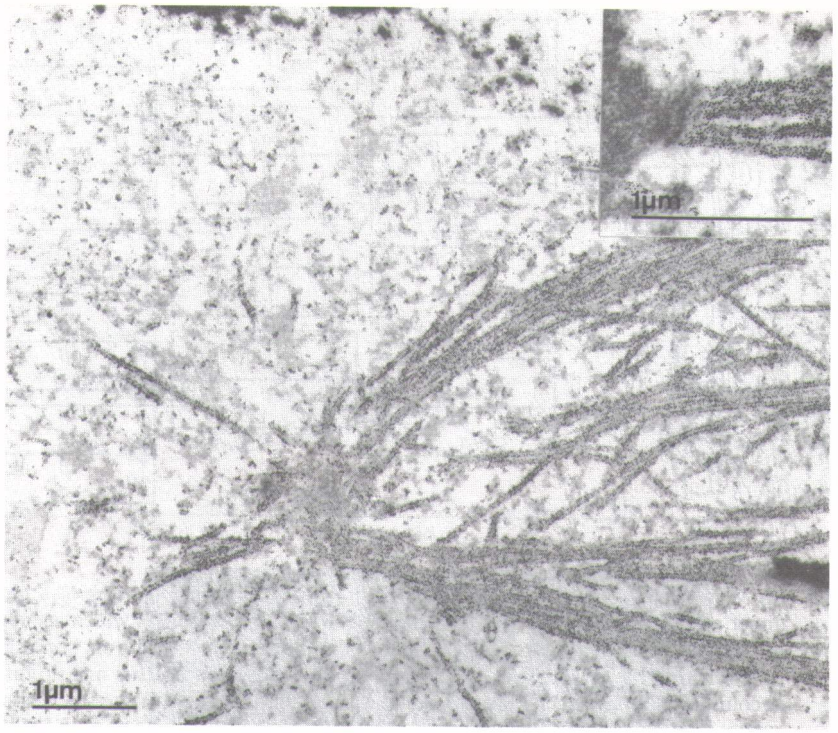

FIGURE 2. MTs labeled with tyrosine tubulin immunogold in tissue culture cell during mitosis. Mitotic spindle MTs emanate from centrioles at left. Insert upper right: MTs attaching to chromosomes. With permission from Geuens *et al.* (1986).

MICROTUBULES

MTs are polymer assemblies of subunit proteins called tubulin. Each tubulin is a 110 kDa barbell-shaped dimer 4 nm × 4 nm × 8 nm, consisting of an alpha and a beta monomer (Amos & Klug, 1974). Linked end to end, the tubulin dimers comprise chain-like protofilaments; 13 protofilaments laterally associated form an MT—hollow cylinders 25 nm in diameter with lengths ranging from nanometers to millimeters in some neuronal cells (Figure 3(a)). The tubulin subunits within MT walls are arranged in a skewed hexagonal lattice and the MTs have a local and a net polarity due to a positive charge on beta monomers and a negative charge on alpha monomers. MAPs attach at specific subunit sites and interconnect MTs with other MTs, cytoskeletal elements (i.e. actin, intermediate filaments, membrane-connecting proteins) and organelles to form dynamic networks. These radiate from perpendicular pairs of centrioles, supercylinders comprised of MT doublets. Often nucleated by negatively charged alpha ends at centrioles, MT assembly can also occur freely in cytoplasm without nucleation. The assembly occurs preferentially at positively charged MT beta ends (DeBrabander *et al.*, 1986). The density and complexity of cytoskeletal MT networks, sub-networks, and their associated bound water molecules indicate that eukaryotic cell interiors have a large solid-state component which can interchange with the liquid phase. This supports theoretical findings (Langton, 1990) that biological systems operate at or near a solid−fluid (sol−gel) phase transition.

MT assembly is believed to be an entropy-driven process partly because the unpolymerized subunits bind and order more water molecules than do the assembled MTs (Dustin, 1984).

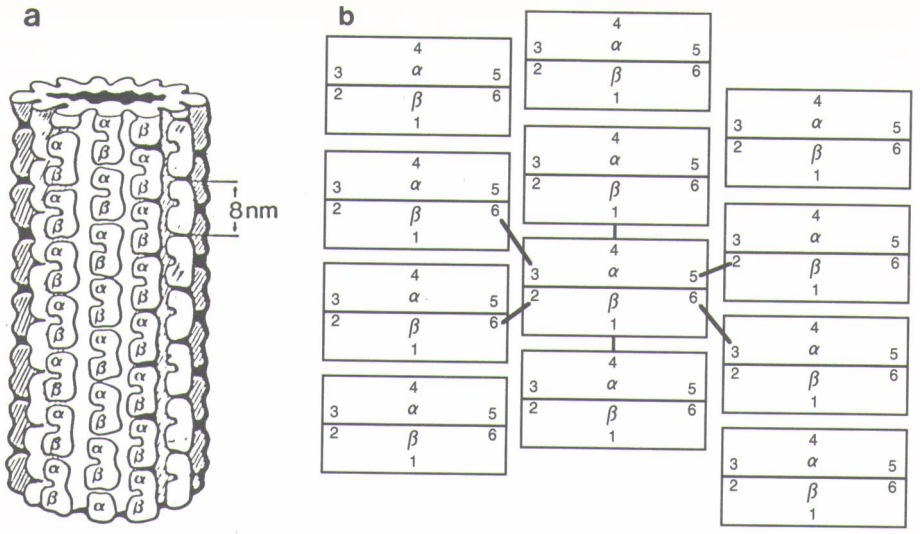

FIGURE 3. (a) MTs are cylinders whose walls are 13 protofilaments, each a string of 8 nm tubulin dimer subunits. Alpha and beta tubulin monomers form the dimers which also bind GTP or GDP. (b) Tubulin dimers defined as movable finite automaton with six bond sites. MTs represented as a two-dimensional lattice with tubulin dimers in rows and protofilaments in columns. The same geometry is used to define the MT lattice for the stochastic cellular automaton. Note the skewed hexagonal lattice geometry: one-and-a-half dimers per circumference. The alpha end of an MT is referred to as the 'north end' and the beta end is referred to as the 'south end'.

Both polymerized and unpolymerized subunits bind either GTP or GDP (high energy phosphate bond containing analogues of ATP and ADP). Energy is imparted to the tubulin subunits by the hydrolysis of GTP to GDP; however, the hydrolysis energy is not required for assembly. Rather, GTP hydrolysis to GDP occurs subsequently within assembled MTs. (Utilization of the hydrolysis energy is not understood, but has been suggested to change bond strengths and/or contribute to generation of coherent lattice excitations, phonons or solitons within MTs.) GTP and GDP binding impart different and distinct conformational states of tubulin (Carlier, 1983).

Adaptive cell activities apparently utilize a particular type of MT assembly/disassembly described *in vitro* as 'dynamic instability' (Kirschner & Mitchison, 1986). In dynamic instability, MTs are labile structures which can alternate erratically between growing and rapidly shrinking phases (Figure 4). Whether growing or shrinking occurs depends on a variety of factors, including the presence of stabilizing MAPs, concentrations of ions (i.e. Ca^{++}, Mg^{++}), availability of free GTP tubulin and the rate of hydrolysis of GTP tubulin to GDP tubulin within assembled MTs. The latter is important because MTs whose ends are comprised of GTP tubulin (GTP 'caps') are stable; those whose ends have exposed GDP tubulin are unstable and disassemble rapidly. Consequently, if the addition of free GTP tubulin matches or exceeds the rate of GTP hydrolysis within MTs, a GTP 'cap' protects the growing MT end. As MTs grow and consume free GTP tubulin, available free GTP tubulin may drop below a critical value and the rate of assembly drops. As intra-MT hydrolysis of GTP tubulin to GDP tubulin continues, the GTP tubulin cap is lost, GDP tubulin is exposed at the MT end, and rapid disassembly occurs. The disassembly yields abundant free GDP tubulin which is reconverted to free GTP tubulin, promoting reassembly. In the absence of stabilizing factors

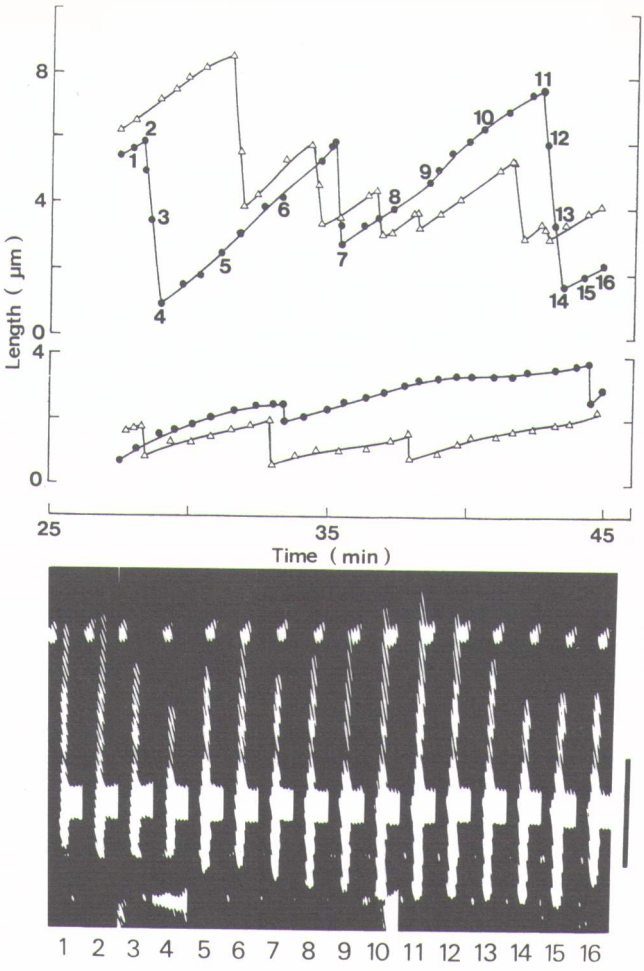

FIGURE 4. Direct observation of MTs growing and shrinking (Horio & Hotani, 1986). The distance between both ends of a single MT and a fixed point on the MT was measured. The top graph shows the distance of the more active (presumably beta plus) MT end from the fixed point, and the middle graph shows the distance of the less active (presumably alpha minus) end from the fixed point. Curves represented by dots and triangles denote two different, specific MTs. The bottom graph shows the dark-field video microscopy sequence corresponding to the lengths of the MTs denoted by dots in the top and middle graphs. The more active end is on top. Scale bar is 5 μm.

such as MAPs, centrioles or other structures, switching between phases of MT assembly and disassembly occurs.

The two ends of MTs apparently differ in their assembly/disassembly characteristics because the positively charged beta ends bind GTP tubulin more strongly than do the negatively charged alpha ends. Consequently, within narrow ranges of unpolymerized GTP tubulin concentration and rate of GTP hydrolysis within MTs, and when dynamic instability is suppressed by the presence of MAPs, assembly at the beta end may equal disassembly at the alpha end. This results in a steady state of dynamic MTs of constant length, i.e. treadmilling (Figure 5), as opposed to the dynamic instability transition phenomenon.

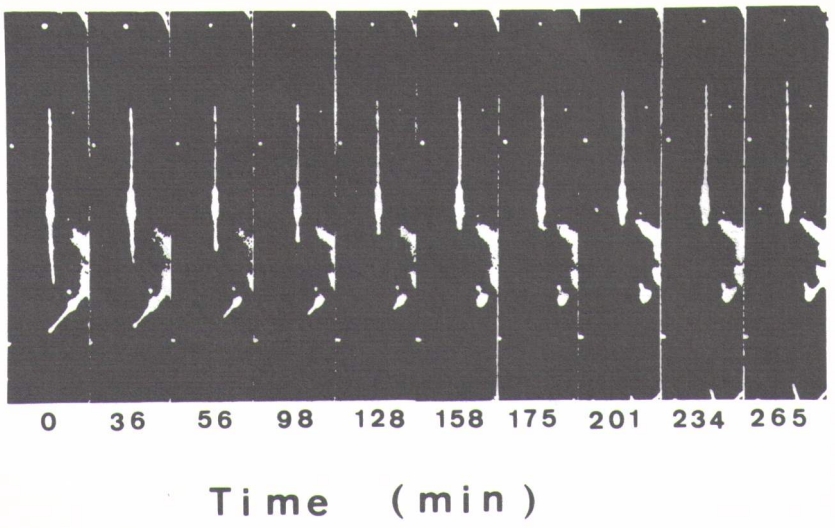

FIGURE 5. Direct observation of treadmilling. An MT of near constant length with a marker (thickened area—immunofluorescent MAP) 'moving' through it. This illusion occurs because MT assembly is occurring at the top end, and disassembly at the bottom. Scale bar is 5 μm.

Stable cytoskeletal networks are anchored within cells by attachment to centrioles, MAPS and other cytoskeletal structures, including membrane connections. Cells may use rapid switching between assembly and disassembly (dynamic instability) in growth, movement, adaptive probing and extension of diverse cellular processes such as amoeboid pseudopodia, and neural axonal and dendritic growth cones.

DIRECT OBSERVATION OF MICROTUBULE ASSEMBLY/DISASSEMBLY AND LIPOSOME–MICROTUBULE INTERACTIONS

Predictions of dynamic instability and treadmilling (Kirschner & Mitchison, 1986) based on experimental data have been confirmed by direct observation of individual MT assembly/disassembly using dark-field video microscopy (Horio & Hotani, 1986). Tubulin was isolated from calf brains by three cycles of temperature-dependent assembly/disassembly (Sloboda *et al.*, 1975) and further purified by phosphocellulose column chromatography (Sloboda *et al.*, 1976). Assembly of MTs was initiated by raising the temperature from 0°C to 37°C in a 1.7 mg ml^{-1} tubulin solution in buffer (90 mM PIPES, 1.8 mM EGTA, 0.9 mM $MgSO_4$, 2.7 mM GTP, pH 6.9). After incubation for 2 min, 4 μl of the solution was transferred onto a slide glass, mounted with a coverslip (22 mm × 22 mm) and observed by dark-field microscopy, with which individual MTs could be monitored. Tubulin concentration (1.7 mg ml^{-1} or 0.015 mM) was greatly exceeded by the concentration of GTP (2.7 mM) so that all free tubulin may be considered to be GTP tubulin.

Real-time video recording revealed that both ends of MTs exist in either growing phase or shortening phase, and switch frequently between the two phases in an erratic, seemingly chaotic manner (Figure 4). In certain cases, growing and shortening ends are observed to coexist on the two ends of a single MT, one end growing and the other end shrinking (treadmilling—Figure 5). In the presence of MAPs it is observed that MT disassembly at both ends is interrupted recurrently, after which the disassembly resumes.

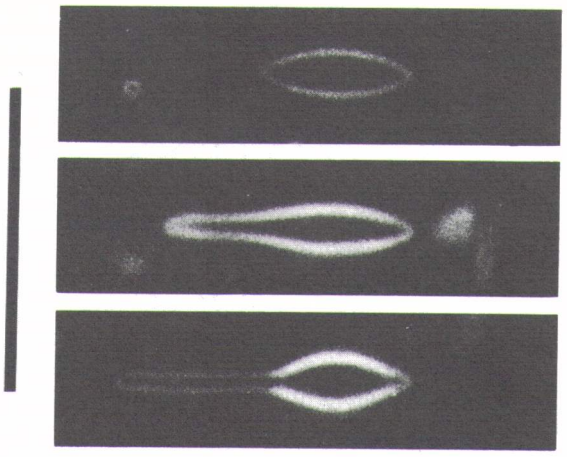

FIGURE 6. Liposome within which MTs are assembling. MT growth causes deformation and extension of membrane. Scale bar is 5 μm.

The rate of MT growth reached 0.63 μm min^{-1} (10 nm s^{-1}, or about one row of tubulin dimers per second) at the active (positively charged beta) end and about one-third of that at the inactive (negatively charged alpha) end. The rate of disassembly was maximal at the negatively charged alpha end (about 20 tubulin dimer rows per second) and slower (about 10 tubulin dimer rows per second) at the positively charged beta end.

To study the role of the cytoskeleton in the morphogenesis of biological cells, liposomes containing tubulin were prepared. Phospholipid molecules in solution can assemble spontaneously into membranous bilayer structures, similar to biological membranes. These membranous structures spontaneously form closed spherical vesicles called liposomes. To make a liposome containing tubulin, mixed dry lipid composed of dimyristoyl-phosphatidylcholine and phosphatidylglycerol (1:1 in molar ratio) was suspended in a tubulin solution. Many spherical liposomes were formed by incubation for 10 min at 10°C. The liposome–tubulin solution was diluted fourfold to prevent microtubule formation outside the liposomes. The concentration of tubulin inside the liposomes remained constant because tubulin does not pass through liposome membranes. An increase in temperature to 24°C resulted in polymerization of tubulin within the liposomes. The morphological changes of a liposome were observed by high intensity dark-field microscopy (Figure 6). As the length of the MTs increased within it, a spherical liposome changed into a football shape, and then two straight tubes started to grow at both ends of the football. The morphogenesis of this bipolar shape indicates that polymerization of tubulin can generate enough mechanical force to deform a membrane vesicle. Apparently similar phenomena are observed *in vivo* at the growing edge of an axon growth cone, although actin and other cytoskeletal structures may interpose between MTs and membranes (Smith, 1988).

STOCHASTIC CELLULAR AUTOMATA MODEL OF MICROTUBULE ASSEMBLY/DISASSEMBLY

To simulate MT asssembly/disassembly, we have used two types of cellular automata. In a simple stochastic cellular automata model, the relation between bound and free tubulin and water is discussed. Each tubulin subunit can be considered to be in one of five different states: as polymerized tubulin with attached MAPs (0); as polymerized tubulin dimers with either GTP (1) or GDP (2); as free tubulin with either GDP (3), or GTP (4). State 5 represents

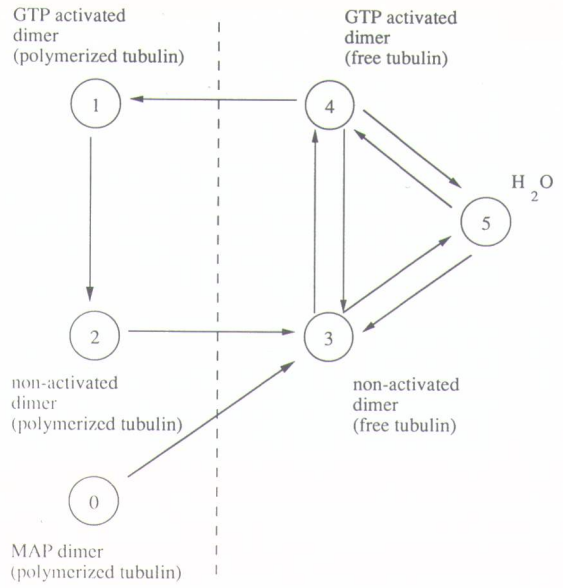

FIGURE 7. State diagram for a simple stochastic CA model of MT. State O is tubulin dimer in polymerized form (MT geometry) with an MT attached protein (MAP). State 1 is GTP-activated MT tubulin. State 2 is MT tubulin in non-activated form (GDP), state 3 is non-activated free dimer (in solution), state 4 is GTP-activated free dimer (in solution), and state 5 is water. The transitions are discussed in the text. Note that the transitions between the states 3, 4 and 5 simulate physical replacement processes whereas all other transitions simulate physical transitions between different states of a particular tubulin molecule. Also note that this model is formulated partly as a Markov chain and partly as a cellular automaton.

water. The possible transitions are shown in Figure 7. States 0−2 model tubulin in MT geometry and states 3−5 model the solution including water. Note that the transitions between states 3, 4 and 5 simulate physical replacement processes and all other transitions simulate physical transitions between different states of particular tubulins. The automaton is defined on a two-dimensional lattice (Figure 3(b)) where protofilaments are represented in columns (i). In the MT structure a dimer (i,j) is surrounded by six neighboring dimers labeled with different orientations—north, northeast, southeast, south, southwest, northwest (N, NE, SE, S, SW, NW)—in agreement with previously described nomenclature (Hameroff *et al.*, 1989; Rasmussen *et al.*, 1990). The modeling of simple elongation and shrinking of MT using this approach is described in Rasmussen *et al.*, 1990.

We shall now model (i) the observed stepwise disassembly process associated with dynamic instability, and (ii) the observed treadmilling phenomena.

We assume that the GTP hydrolysis to form GDP tubulin occurs through a non-linear process 1→2 described by some probability P_{12} which depends on the states of the neighboring sites and on the concentration of free tubulin. When the majority of neighbors (three or more) are in the polymerized GTP state (state 1), $P_{12} = 0$. Otherwise, P_{12} has a finite value determined by the concentration of free tubulin. Such a mechanism ensures an enduring GTP cap.

The MT disassembly 2→3 occurs through disassembly of polymerized GDP tubulin (state 2). This process is assumed to depend on its location at the MT boundary. A polymerized boundary dimer will go into solution with a finite probability P_{23} if three or more of its neighbors are of the free GTP tubulin or water states. Different disassembly rates at the negatively charged alpha ends and at the positively charged beta ends are obtained by using

different disassembly probabilities $P_{23\alpha}$ and $P_{23\beta}$ ($P_{23\alpha} < P_{23\beta}$) at the two ends. To determine in which end a particular boundary dimer is can be done technically by checking in which states the northern and southern neighbors are.

A tubulin subunit with an attached MAP, state 0, is more strongly bound to the MT. The disassembly process, $0 \rightarrow 3$, will therefore only take place if three or more of its neighbors are in unpolymerized form with some small probability P_{03}. The smaller P_{03} is, the more discontinuous is the overall disassembly process expected to be for MTs with MAPs.

In this model, the concentrations of the GTP tubulin and the GDP tubulin are determined by a stochastic process involving internal transitions between the three states 3, 4 and 5. The higher the overall probability for the presence of a GTP tubulin among the free states, the more likely it is that a polymerization will take place in the system. The polymerization $4 \rightarrow 1$ will occur with probability P_{41} if a GTP tubulin is aligned with at least two GTP tubulin subunits. Different assembly rates are obtained at the negatively charged alpha ends compared with the positively charged beta ends using different assembly rates $P_{14\alpha}$ and $P_{14\beta}$.

Simulations of MT disassembly with MAPs (state 0) exhibit a discontinuous disassembly rate similar to that which is observed experimentally. The disassembly dynamics for this phenomenon are shown in Figures 8(A) and 8(B). Figure 8(C) shows treadmilling, a steady state phenomenon. Both simulations assume constant concentrations of free GTP tubulin. Since it is a linear Markov chain (states 3, 4 and 5) that determines the probability at each time step of a collision between a GTP-activated dimer in solution and a boundary dimer in MT geometry, the probability of a reactive collision per unit time for any set of parameters can be calculated analytically (Cox & Miller, 1978). Alternatively, if the frequency of a reactive collision is known, the corresponding parameters can also be derived.

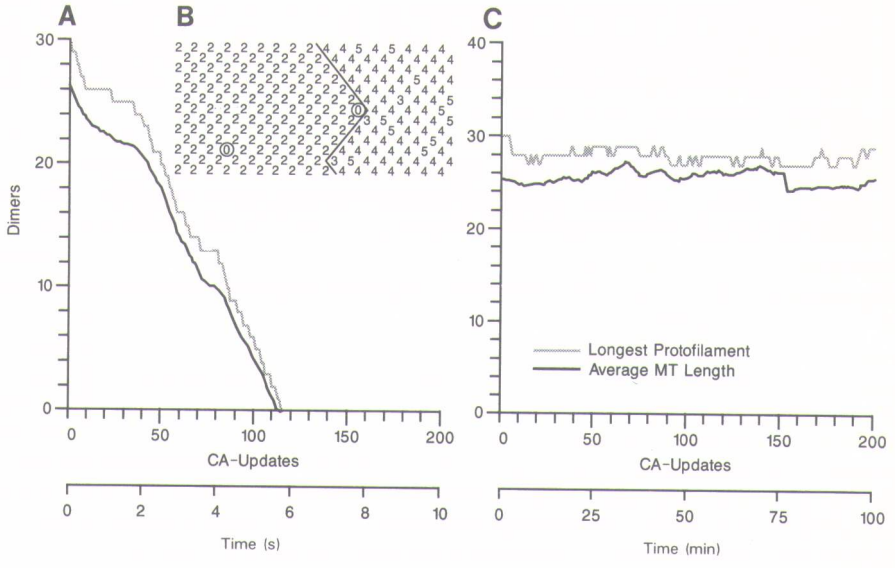

FIGURE 8. (A) Disassembly. The MT length (number of dimers) as a function of time. The length is measured as the longest protofilament in the MTs at any time. The erratic rate indicates that the disassembly gets 'stuck' every time dimers associated with an MAP are at the free ends. These dimers are less likely to get disassembled. (B) The molecular situation when the disassembly is temporarily blocked 'around' the 0-state (the MAP dimer state) since this dimer only goes into sulution with low probability. (C) Treadmilling. The MT length (number of dimers) as a function of time. The length is virtually constant while assembly is occurring at the beta end and disassembly is occurring at the alpha end.

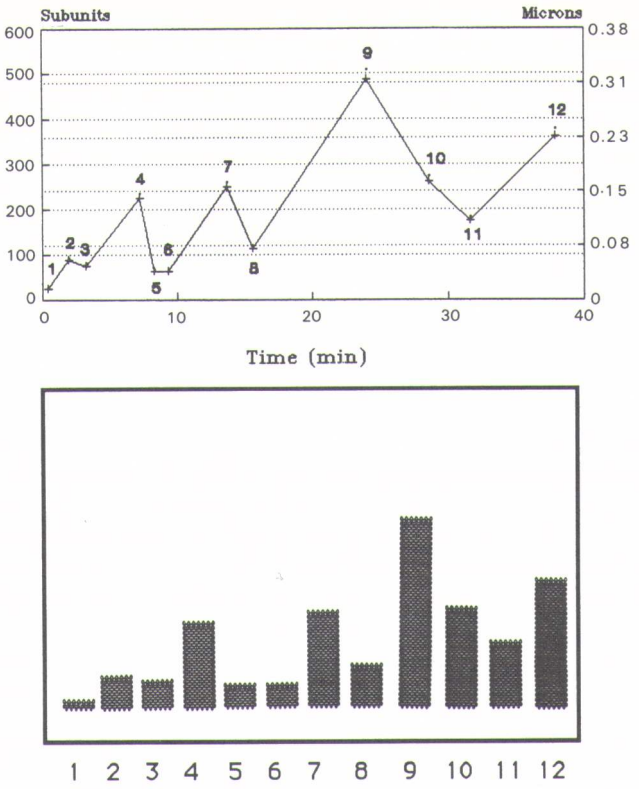

FIGURE 9. MFA simulation of the change in MT length (number of polymerized subunits) measured at different times. Top: graphic plot of MT length versus time at dynamic instability. Bottom: MT automaton simulations at 12 times the scale of the top part. Note similarity to Figure 4.

The clocking frequency for the model is tuned to match the dynamics of the experimental observations. In the disassembly simulation (Figures 8(A) and 8(B)), the cellular automaton update time corresponds to approximately 1/20 s, real time. In the treadmilling simulation the cellular automaton clock frequency corresponds to approximately 1/2 min, real time. The treadmilling simulation shown in Figure 8(C) is obtained using the following parameters: $P_{12} = 0.60$, $P_{23\alpha} = 0.72$, $P_{23\beta} = 0.75$, $P_{34} = 0.7$, $P_{35} = 0.1$, $P_{41\alpha} = 0.9$, $P_{41\beta} = 0.9$, $P_{43} = 0.05$, $P_{45} = 0.1$, $P_{53} = 0.15$, and $P_{54} = 0.75$. To calculate the steady state distribution of the molecules in solution, P(state 3), P(state 4) and P(state 5), we assume that the net transitions between all states in solution are zero. One such condition is that P(state 3) $\times P_{34} = P$(state 4) $\times P_{43}$. Thus, the steady state probabilities are 0.11, 0.06 and 0.83 respectively. This implies, for instance, that the probability of a reactive collision between a free activated dimer and an MT-activated dimer is P(state 4) $\times P_{41} = 0.83 \times 0.90$ per cellular automaton update. The expected number of reactive collisions per cellular automaton update is therefore 13×0.75. This corresponds to $0.5 \times 9.71 \simeq 4.86$ reactions per minute real time. In the disassembly simulation shown in Figure 8(A) the parameters are as in Figure 8(C) except that $P_{03} = 0.02$, $P_{23\alpha} = 0.75$ and $P_{23\beta} = 0.35$.

To model the initial nucleation process of the MT assembly and other processes where no predefined 'lattice' exists, the technique of movable finite automata becomes more appropriate. Movable finite automata are also suitable to model more detailed molecular properties, since important biophysical parameters can be modeled more explicitly.

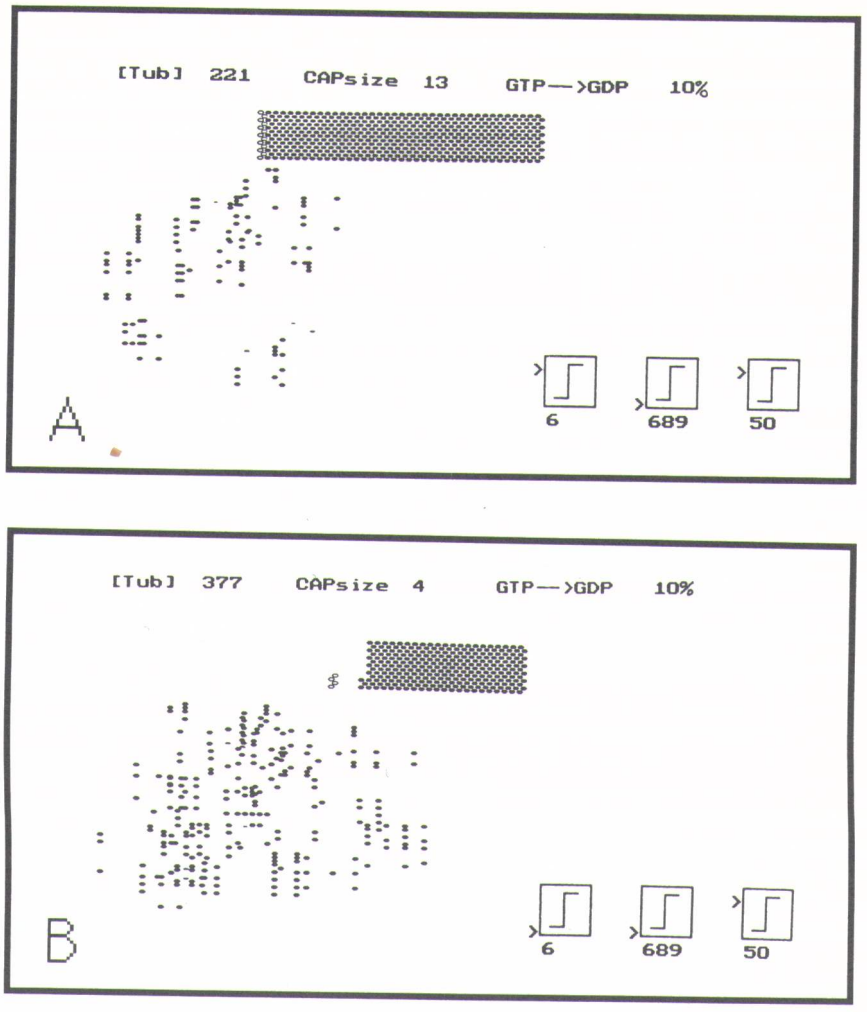

FIGURE 10. MT assembly/disassembly simulation. Critical values: cap_{crit} = 6 dimers [$tubulin_{high}$] = 689 dimers, [$tubulin_{low}$] = 50 dimers. (A) MTs grow until the free GTP tubulin concentration is below 50 subunits, otherwise growth takes place until the GTP cap size is less than or equal to 6 GTP subunits. (B) MT shrinking triggered by the cap size. The shrinking process will take place until the free tubulin concentration equals or exceeds 689 dimers. The simulation takes place with a GTP hydrolysis rate of 10% per automaton time step for the tubulin in MT geometry.

MOVABLE FINITE AUTOMATA MODEL OF MICROTUBULE ASSEMBLY/DISASSEMBLY

MT assembly/disassembly can also be simulated using the technique of movable finite automata (MFA) (Thompson & Goel, 1988). In this approach, a protein assembly is modeled as a cellular automaton in which each subunit has a number of bond sites which correspond to neighboring subunit attachments. Applying the technique of MFA to MT geometry (Figure 3(b)), each tubulin dimer is defined as an automaton subunit with six bond sites labeled 3, 4 and 5 on the alpha monomer, and 1, 2 and 6 on the beta monomer. Bond site relationships between

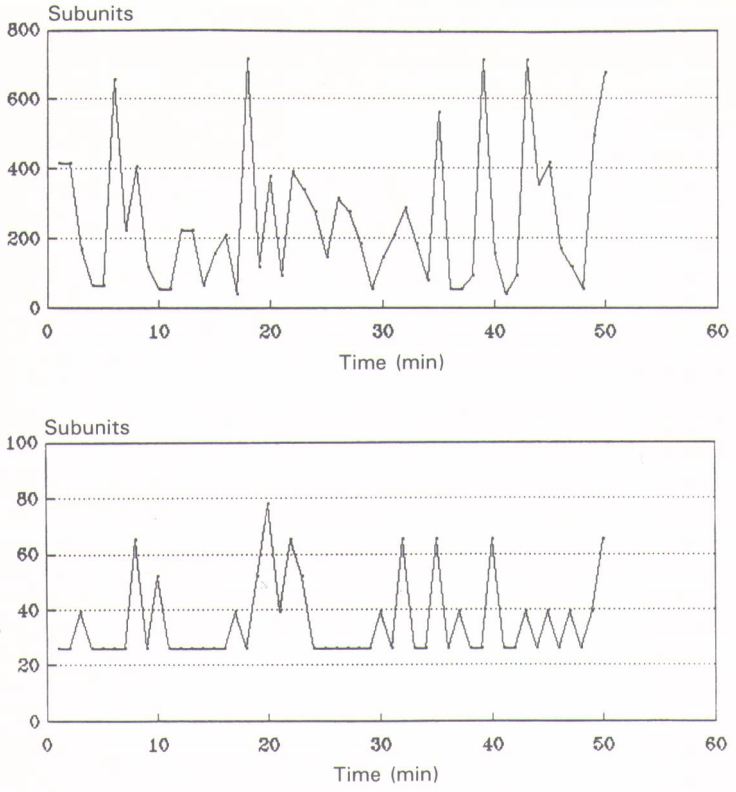

FIGURE 11. Oscillations of MT length (number of subunits polymerized) are related to the GTP hydrolysis rate. The oscillatory behavior of MT assembly is partially explained by the GTP cap size which depends on this rate. MT assembly takes place until the cap size reaches a critical value cap_{crit}. The figure shows results obtained in two simulations at 50 different times with $cap_{crit} = 8$ dimers, $[tubulin_{low}] = 25$ dimers, but different GTP hydrolysis rates. Top: GTP hydrolysis = 5% of terminal subunits per automaton update. Bottom: GTP hydrolysis = 50% of terminal subunits per automaton update.

assembled dimers are fixed due to the geometry of the MT lattice. Thus, for example, the $\alpha 5$ site on one subunit is adjacent to the $\beta 2$ site on its neighboring subunit.

In the present study, we utilize two different tubulin subunit conformational states determined by the binding of either GTP or GDP (Carlier, 1983). The GTP tubulin conformation binds more strongly at neighbor tubulin attachment sites, promoting assembly, whereas the GDP tubulin conformation binds neighbor tubulins only loosely, promoting disassembly. Thus, hydrolysis of GTP tubulin to GDP tubulin within MTs imparts a tubulin conformational state change with lowered affinities, so promoting disassembly. Independent of assembled tubulin GTP versus GDP states on the MT lattice, a low concentration of free GTP tubulin prevents assembly and promotes disassembly. Also independent of the assembled tubulin GTP versus GDP states, a high concentration of free GTP tubulin prevents disassembly and promotes assembly. It should be noted that these mechanisms enable the system to exhibit hysteresis.

Applying the MFA technique to MT assembly/disassembly, transitions between dynamic instability phases (growth and shrinking) are controlled by the free GTP tubulin concentration, the GTP cap size and the rate of polymerized GTP tubulin hydrolysis (Figures 9–11). If the free GTP tubulin concentration is below or equal to a critical low value $[tubulin_{low}]$, MT shrinking occurs; if the free GTP tubulin concentration is above or equal to a critical

high value [$tubulin_{high}$], MT growth occurs. In the present simulations, [$tubulin_{low}$] = 50 dimers in solution and [$tubulin_{high}$] = 689 dimers in solution. The total number of tubulin molecules in both MT geometry and solution is 715. Under normal circumstances (recall the experimental conditions in the section on direct observation of MT assembly/disassembly), free GDP tubulin is readily converted to free GTP tubulin, so this step is not rate limiting and therefore not modeled. If the free GTP tubulin concentration is in the range between these high and low values, then the GTP tubulin cap size determines whether growth or shrinking occurs. Within this range, if the cap size is above a critical value cap_{crit}, MT growth occurs (Figure 10(A)); if the cap size is below or equal to cap_{crit}, MT shrinking occurs (Figure 10(B)).

The GTP tubulin cap size in our simulation considers only the terminal row of tubulin dimers with a maximal size of 13, one dimer per protofilament. In the illustrated simulation, cap_{crit} = 6 dimers. The GTP cap size is determined by the addition of GTP tubulin during growth (which increases the GTP cap size) and the hydrolysis of GTP tubulin to GDP tubulin within MTs (which decreases the GTP cap size). With some probability predefined at the beginning of the simulation (10% per automaton update in the illustrated case), each of these GTP tubulin dimers may be hydrolyzed to GDP tubulin. If the number of GTP tubulin dimers in the terminal row is less than or equal to cap_{crit}, shrinking occurs if free GTP tubulin is below [$tubulin_{high}$]. If the number of GTP tubulin in the terminal row is greater than cap_{crit}, growth occurs if free GTP tubulin is above [$tubulin_{low}$]. Typical simulation results showing erratic growing and shrinking are shown in Figure 9; measured over time, these simulation results strongly resemble experimental results (Figure 4) obtained by Horio & Hotani (1986) using dark-field microscopy. Figure 11 shows MT assembly/disassembly oscillation behavior dependent on the rate of GTP hydrolysis.

DISCUSSION

This paper describes *in vitro* observation and two types of computerized cellular automata simulation of MT assembly/disassembly dynamics. The *in vitro* studies of individual MT dynamics show erratic oscillations between phases of assembly and disassembly (dynamic instability), simultaneous assembly and disassembly at either end of a single MT of a relatively constant length (treadmilling), discontinuous disassembly in the presence of MAPs, and assembly within liposomes which deform and extend the liposome walls.

MT assembly within liposomes considers two essential ingredients of biological cells. Artificial liposomes have been used as therapeutic drug-release systems when filled with a drug and injected into patients (Gregoriadis, 1988). Liposomes filled with hemoglobin can function for several hours in humans as artificial red blood cells (Farmer *et al.*, 1988; Djordjevich & Ivankovich, 1988). Liposomes, however, are passive and incapable of motor or adaptive behavior. Our *in vitro* studies describe cytoskeletal MT polymerizing within liposomes, causing marked deformation and extension of the liposome surface. Such artificial 'pseudopodia' may herald more dynamic functions. With a cytoskeletal regulation system, genetic and other components may be selectively added or allowed to evolve, leading to future complex and functional artificial cells (Chang, 1988).

In the stochastic cellular automaton MT simulation, inclusion of MAPs causes a discontinuous disassembly phase, reproducing the *in vitro* results. The observed treadmilling phenomena can also be reproduced by the simple stochastic cellular automata. The movable finite automaton model exhibits both treadmilling (not shown) and erratic oscillations between assembly and disassembly phases (dynamic instability), again reproducing *in vitro* results. The dynamics of the GTP cap are modeled differently in the two approaches. In the stochastic cellular automaton approach discussed earlier, the cap size can vary over several dimers whereas the MFA model, also discussed earlier, only considers the last dimer row. However, both models exhibit approximately the same cap dynamics. In the MFA model, we have introduced a feedback between tubulin in MT geometry and tubulin in solution which enables

us to obtain the dynamic instability phenomena of erratic shrinking and growth. In the stochastic model, we assume a constant tubulin concentration which precludes oscillatory assembly dynamics. The simulations sufficiently match the *in vitro* observations to justify acceptance of the roles of the critical parameters chosen: free GTP tubulin concentration, GTP cap size, GTP−GDP hydrolysis rate, and presence of MAPs. Living cells utilize these phenomena in real-time adaptive behavior (cell growth, movement, axonal and dendritic extension, synapse formation etc.), suggesting that these *in vitro* studies and simulations capture some of the logic and basic elements of adaptive cytoskeletal behavior.

REFERENCES

Amos, L.A. & Klug, A. (1974) Arrangement of subunits in flagellar microtubules. *Journal of Cellular Science* **14,** 523−550.

Carlier, M.F. (1983) Kinetic evidence for a conformation change of tubulin preceding microtubule assembly. *Journal of Biological Chemistry* **258,** 2415−2420.

Chang, T.M.S. (1988) Artificial cells with ultrathin lipid-polymer or lipid-protein membranes. *Advances in Experimental Medicine and Biology* **238,** 251−223,

Cox, D.R. & Miller, H.D. (1978) *The Theory of Stochastic Processes,* Chapman and Hall, London.

DeBrabander, M., Geuens, G., Demey, J. & Joniav, M. (1986) The organized assembly and function of the microtubule system throughout the cell cycle, in *Cell Movement and Neoplasia* (DeBrabander, M., Ed.) Pergamon Press, Oxford, pp. 29−40.

Djordjevich, I. & Ivankovich, A.D. (1988) Progress in development of synthetic erythrocytes made by encapsulation of hemoglobin. *Advances in Experimental Medicine and Biology* **238,** 171−197.

Dustin, P. (1984) *Microtubules* (2nd revised edn). Springer, Berlin.

Farmer, M.C., Johnson, S.A., Beissenger, R.L., Gossage, J.L., Lynn, A.B. & Carter, K.A. (1988) Liposome-encapsulated hemoglobin. *Advances in Experimental Medicine and Biology* **238,** 161−170.

Geuens, G., Gundersen, G.G., Nuydens, R., Cornellisen, F., Bulinski, J.C. & DeBrabander, M. (1986) Ultrastructural co-localization of tyrosinated and un-tyrosinated alpha-tubulin in interphase and mitotic cells. *Journal of Cell Biology* **103,** 1883−1893.

Gregoriadis, G. (1988) Liposomes as a drug delivery system. *Advances in Experimental Medicine and Biology* **238,** 151−159.

Hameroff, S.R. (1987) *Ultimate Computing: Biomolecular Consciousness and Nanotechnology.* North-Holland Amsterdam.

Hameroff, S.R., Rasmussen, S. & Mansson, B. (1989) Molecular automata in microtubules: basic computational logic of the living state?, in *Artificial Life: Proceedings of an Interdisciplinary Workshop on the Simulation, Origin and Representation of Living Systems* (Langton, C., Ed.) Addison Wesley, Santa Fe Institute, pp. 521−553.

Horio, T. & Hotani, H. (1986) Visualization of the dynamic instability of individual microtubules by dark field microscopy. *Nature (London)* **321,** 605−607.

Kirschner, M. & Mitchison, T. (1986) Beyond self-assembly: from microtubules to morphogenesis. *Cell* **45,** 329−342.

Langton, C.G. (1990) Computation at the edge of chaos: phase transitions and emergent computation. *Physica D* **42,** 12−37.

Lennon, A.M., Francon, J., Fellous, A. & Nunez, J. (1980) Rat, mouse, and guinea-pig brain development and microtubule assembly. *Journal of Neurochemistry* **35,** 804−813.

Rasmussen, S., Karampurwala, H., Vaidyanath, R., Jensen, K.S. & Hameroff, S. (1990) Computational connectionism within neurons: a model of cytoskeletal automata subserving neural networks. *Physica D* **42,** 428−449.

Sloboda, R.D. *et al.* (1976) in *Cell Motility* (Goldman, R., Pollard, T., & Rosenbaum, J., Eds) Cold Spring Harbor Laboratory, New York, pp. 1171−1212.

Sloboda, R.D., Rudolph, S.A., Rosenbaum, J.L. & Greengard, P. (1975) *Proceedings of the National Academy of Sciences, USA* **72(1),** 177−181.

Smith, S.V. (1988) Neuronal cytomechanics: the actin-based motility of growth cones. *Science* **242,** 708−715.

Thompson, R.L. & Goel, N.S. (1988) Movable finite automata (MFA) models for biological systems I: bacteriophage assembly and operation. *Journal of Theoretical Biology* **131,** 351−385.